

## Fast and accurate clothoid fitting

ENRICO BERTOLAZZI and MARCO FREGO, University of Trento, Italy

An effective solution to the problem of Hermite  $G^1$  interpolation with a clothoid curve is provided. At the beginning the problem is naturally formulated as a system of nonlinear equations with multiple solutions that is generally difficult to solve numerically. All the solutions of this nonlinear system are reduced to the computation of the zeros of a single nonlinear equation. A simple strategy, together with the use of a good and simple guess function, permits to solve the single nonlinear equation with a few iterations of the Newton–Raphson method.

The computation of the clothoid curve requires the computation of Fresnel and Fresnel related integrals. Such integrals need asymptotic expansions near critical values to avoid loss of precision. This is necessary when, for example, the solution of interpolation problem is close to a straight line or an arc of circle. Moreover, some special recurrences are deduced for the efficient computation of asymptotic expansion.

The reduction of the problem to a single nonlinear function in one variable and the use of asymptotic expansions make the solution algorithm fast and robust.

Categories and Subject Descriptors: G.1.2 [Numerical Analysis]: Approximation

General Terms: Algorithms, Performance

Additional Key Words and Phrases: Clothoid fitting, Fresnel integrals, Hermite  $G^1$  interpolation, Newton–Raphson

### ACM Reference Format:

Enrico Bertolazzi, Marco Frego. Fast and accurate clothoid fitting ACM Trans. Math. Softw. V, N, Article A (January YYYY), 14 pages.

DOI = 10.1145/0000000.0000000 <http://doi.acm.org/10.1145/0000000.0000000>

## 1. INTRODUCTION

There are several curves proposed for Computer Aided Design [Farin(2002); Baran et al.(2010)Baran, Lehtinen, and Popović; De Boor(1978)], for planning trajectories of robots and vehicles or the geometric design of roads [De Cecco et al.(2007)De Cecco, Bertolazzi, Miori, Oboe, and Baglivo; Scheuer and Fraichard(1997)]. The most important among these are clothoids also known as Euler’s or Cornu’s spirals, clothoids splines, i.e. a planar curve consisting in clothoid segments, circles and straight lines, [Davis(1999); Meek and Walton(1992); Meek and Walton(2004); Meek and Walton(2009); Walton and Meek(2009)], generalized clothoids or Bezier spirals [Walton and Meek(1996)]. Pythagorean Hodograph [Walton and Meek(2007); Farouki and Neff(1995)], bi-arcs and conic curves are also widely used [Pavlidis(1983)]. It is well known that the best or most pleasing curve is the clothoid, despite its transcendental form.

The procedure that allows a plane curve to interpolate two given points with assigned (unit) tangent vectors is called  $G^1$  Hermite interpolation, if given curvatures at the two points is also satisfied, then this is called  $G^2$  Hermite interpolation [McCrae and Singh(2009)]. A single clothoid segment is not enough to ensure  $G^2$  Hermite interpolation, because of the insufficient degrees of freedom. Many authors have provided algorithms that use a pair of clothoids segments to reach the  $G^2$  Hermite interpolation requests. However,

---

Author’s addresses: Department of Mechanical and Structural Engineering

Permission to make digital or hard copies of part or all of this work for personal or classroom use is granted without fee provided that copies are not made or distributed for profit or commercial advantage and that copies show this notice on the first page or initial screen of a display along with the full citation. Copyrights for components of this work owned by others than ACM must be honored. Abstracting with credit is permitted. To copy otherwise, to republish, to post on servers, to redistribute to lists, or to use any component of this work in other works requires prior specific permission and/or a fee. Permissions may be requested from Publications Dept., ACM, Inc., 2 Penn Plaza, Suite 701, New York, NY 10121-0701 USA, fax +1 (212) 869-0481, or [permissions@acm.org](mailto:permissions@acm.org).

© YYYY ACM 0098-3500/YYYY/01-ARTA \$10.00

DOI 10.1145/0000000.0000000 <http://doi.acm.org/10.1145/0000000.0000000>

often it is considered enough the cost-effectiveness of a  $G^1$  Hermite interpolation, because it has been seen numerically that the discontinuity of the curvature is negligible.

The purpose of this paper is to describe a new method for  $G^1$  Hermite interpolation with a single clothoid segment, which does not need to split the problem in mutually exclusive cases as in Meek and Walton(2009), and does not suffer in case of degenerate Hermite data like straight lines or circles (see Figure 1 on the right). These are of course limiting cases but are treated naturally in our approach. Because of numerical stability in the computation, we preferred to introduce an appropriate threshold to avoid such degenerate situation in practice. A precise estimate of such switching points is discussed. Finally, the problem of the  $G^1$  Hermite interpolation is reduced to a solution of a single nonlinear equation, for example by the Newton–Raphson method. In order to provide a fast and accurate algorithm, we give a good initial guess for the Newton–Raphson method solver so that a few iterations suffice.

The remainder of the article is structured as follows. In the next section we define the interpolation problem, in the third we describe the passages to reformulate it such that from three equations in three unknowns it reduces to one nonlinear equation in one unknown. This is enough from the theoretical point of view. The fourth section is devoted to the discussion of a good starting point for the Newton–Raphson method, so that using that guess we achieve a quick convergence, and how to select a correct solution of the nonlinear equation. Section 5 introduces the Fresnel integrals in their standard form and shows how the  $G^1$  interpolation problem (i.e. the argument of the trigonometric functions involved is not purely a second order monomial, but a complete second order polynomial) can be conducted to that form. Section 6 analyzes what happens when the parameters of computation give numerical instabilities in the formulas, and *ad hoc* expressions for such cases are provided. In the appendix there are the algorithms written in pseudo-code and a summary of the algorithm for the accurate computation of the clothoid spline.

## 2. THE FITTING PROBLEM

The construction of highway and railway routes and the trajectories of mobile robots can be split in the in construction of a piecewise clothoid curve which definition is given next.

*Definition 2.1 (Clothoid curve).* The general parametric form of a clothoid spiral curve is the following

$$\begin{aligned} x(s) &= x_0 + \int_0^s \cos\left(\frac{1}{2}\kappa'\tau^2 + \kappa\tau + \vartheta_0\right) d\tau, \\ y(s) &= y_0 + \int_0^s \sin\left(\frac{1}{2}\kappa'\tau^2 + \kappa\tau + \vartheta_0\right) d\tau, \end{aligned} \tag{1}$$

where  $s$  is the arc length,  $\kappa't + \kappa$  is the linearly varying curvature,  $(x_0, y_0)$  is the starting point and  $\vartheta_0$  initial angle. Notice that  $\frac{1}{2}\kappa's^2 + \kappa s + \vartheta_0$  is the angle of the curve at arc length  $s$ .

Clothoids curves are computed via the Fresnel sine and cosine integrals (see Abramowitz and Stegun(1964) for a definition) which is discussed forward in Section 5.

The determination of the parameters  $\vartheta_0$ ,  $\kappa$  and  $\kappa'$  are determined by points and angles at the extrema of the curve. Thus, the problem considered in this paper is stated next.

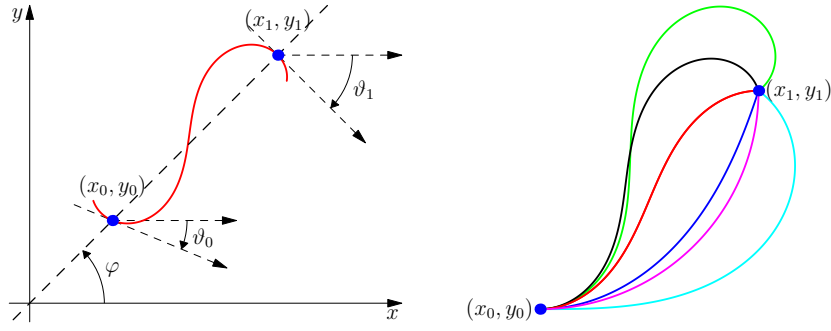


Fig. 1. On the left  $G^1$  Hermite interpolation schema. On the right some cases representing different final angles. The magenta arc is the limiting case of a circle. The other colored arcs represent intermediate cases.

**PROBLEM 1.** Given two points  $(x_0, y_0)$  and  $(x_1, y_1)$  and two angles  $\vartheta_0$  and  $\vartheta_1$ , find a clothoid segment of the form (1) which satisfies:

$$\begin{aligned} x(0) &= x_0, & y(0) &= y_0, & \arctan\left(\frac{y'(0)}{x'(0)}\right) &= \vartheta_0, \\ x(L) &= x_1, & y(L) &= y_1, & \arctan\left(\frac{y'(L)}{x'(L)}\right) &= \vartheta_1, \end{aligned} \quad (2)$$

with minimal positive  $L$  (the length of the curve). The general scheme is showed in Figure 1 on the left.

Solution of Problem 1 is a zero of the following nonlinear system involving the unknowns  $L, \kappa, \kappa'$ :

$$\mathbf{F}(L, \kappa, \kappa') = \begin{pmatrix} x_1 - x_0 - \int_0^L \cos\left(\frac{1}{2}\kappa' s^2 + \kappa s + \vartheta_0\right) ds \\ y_1 - y_0 - \int_0^L \sin\left(\frac{1}{2}\kappa' s^2 + \kappa s + \vartheta_0\right) ds \\ \vartheta_1 - \left(\frac{1}{2}\kappa' L^2 + \kappa L + \vartheta_0\right) \end{pmatrix}. \quad (3)$$

Find the points such that  $\mathbf{F}(L, \kappa, \kappa') = \mathbf{0}$  is a difficult problem to solve in this form. In the next section a reformulation of the problem in a simpler form permits to solve it easily.

### 3. REFORMULATION OF THE PROBLEM

Nonlinear system (3) is put in an equivalent form by introducing the parametrization  $s = \tau L$  so that the integrals involved in computation have fixed extrema independent of  $L$ :

$$\mathbf{F}\left(L, \frac{B}{L}, \frac{2A}{L^2}\right) = \begin{pmatrix} \Delta x - L \int_0^1 \cos(A\tau^2 + B\tau + \vartheta_0) d\tau \\ \Delta y - L \int_0^1 \sin(A\tau^2 + B\tau + \vartheta_0) d\tau \\ \vartheta_1 - (A + B + \vartheta_0) \end{pmatrix}, \quad (4)$$

where  $A = \frac{1}{2}\kappa' L^2$ ,  $B = L\kappa$ ,  $\Delta x = x_1 - x_0$ ,  $\Delta y = y_1 - y_0$ .

The third equation in (4) is linear so that we can solve it with respect to  $B$ ,

$$B = \Delta\vartheta - A, \quad \Delta\vartheta = \vartheta_1 - \vartheta_0, \quad (5)$$

and the solution of nonlinear system (4) is reduced to the solution of the nonlinear system of two equations in two unknown, namely  $L$  and  $A$ :

$$\mathbf{G}(L, A) = \begin{pmatrix} \Delta x - L \int_0^1 \cos(A\tau^2 + (\Delta\vartheta - A)\tau + \vartheta_0) d\tau \\ \Delta y - L \int_0^1 \sin(A\tau^2 + (\Delta\vartheta - A)\tau + \vartheta_0) d\tau \end{pmatrix}, \quad (6)$$

followed by the computation of  $B$  using (5). Nonlinear system (6) is easier to solve than (4). We can perform further simplification using polar coordinates to represent  $(\Delta x, \Delta y)$ , namely

$$\Delta x = r \cos \varphi, \quad \Delta y = r \sin \varphi, \quad (7)$$

and from (7) and  $L > 0$  we can define two new nonlinear functions  $f(L, A)$  and  $g(A)$ , where  $g(A)$  is independent of  $L$ , as follows:

$$f(L, A) = \mathbf{G}(L, A) \cdot \begin{pmatrix} \cos \varphi \\ \sin \varphi \end{pmatrix}, \quad g(A) = \frac{1}{L} \mathbf{G}(L, A) \cdot \begin{pmatrix} \sin \varphi \\ -\cos \varphi \end{pmatrix}.$$

Using the identity  $\sin(\alpha - \beta) = \sin \alpha \cos \beta - \cos \alpha \sin \beta$ , function  $g(A)$  simplifies in:

$$g(A) = \Theta(A; \Delta\vartheta, \Delta\varphi), \quad (8)$$

where  $\Delta\varphi = \vartheta_0 - \varphi$  and

$$\Theta(A; \Delta\vartheta, \Delta\varphi) = \int_0^1 \sin(A\tau^2 + (\Delta\vartheta - A)\tau + \Delta\varphi) d\tau, \quad (9)$$

while using the identity  $\cos(\alpha - \beta) = \cos \alpha \cos \beta + \sin \alpha \sin \beta$ , function  $f(L, A)$  reduces to

$$\begin{aligned} f(L, A) &= \sqrt{\Delta x^2 + \Delta y^2} - L h(A), \\ h(A) &= \int_0^1 \cos(A\tau^2 + (\Delta\vartheta - A)\tau + \Delta\varphi) d\tau = \Theta\left(A; \Delta\vartheta, \Delta\varphi + \frac{\pi}{2}\right). \end{aligned} \quad (10)$$

*Remark 3.1.* Defining  $\phi_0 = \vartheta_0 - \varphi$  and  $\phi_1 = \vartheta_1 - \varphi$  we have  $\Delta\vartheta = \phi_1 - \phi_0$  and  $\Delta\varphi = \phi_0$ , moreover, the angles  $\phi_0$  and  $\phi_1$  are the same used in Walton and Meek(2009) to derive  $G^1$  interpolant.

LEMMA 3.2. *The function  $\Theta$  defined in (9) satisfy*

$$\Theta(A; \Delta\vartheta, z) = 0, \quad \Rightarrow \quad \Theta\left(A; \Delta\vartheta, z + \frac{\pi}{2}\right) \neq 0. \quad (11)$$

PROOF. If  $A = 0$  by a simple computation we obtain

$$\Theta(A; \Delta\vartheta, z) = \begin{cases} \frac{\cos \Delta\vartheta - \cos(\Delta\vartheta + z)}{\Delta\vartheta} & \text{if } \Delta\vartheta \neq 0, \\ \frac{1 - \cos z}{z} & \text{if } \Delta\vartheta = 0, \end{cases}$$

and it is immediate to verify (11). Let  $A > 0$ , after some manipulation we have

$$\frac{\sqrt{2A}}{\sqrt{\pi}} \Theta(A; \Delta\vartheta, z) = (\mathcal{S}(a) + \mathcal{S}(b)) \cos \eta - (\mathcal{C}(a) + \mathcal{C}(b)) \sin \eta$$

where

$$a = \frac{A - \Delta\vartheta}{\sqrt{2\pi A}}, \quad b = \frac{A + \Delta\vartheta}{\sqrt{2\pi A}}, \quad \eta = \frac{\pi}{2} a^2 - z.$$

If implication (11) is false, i.e. both  $\Theta(A; \Delta\vartheta, z) = 0$  and  $\Theta(A; \Delta\vartheta, z + \pi/2) = 0$  then from previous equations it follows

$$\mathcal{S}(a) + \mathcal{S}(b) = 0, \quad \mathcal{C}(a) + \mathcal{C}(b) = 0,$$

and the symmetry  $\mathcal{C}(-z) = -\mathcal{C}(z)$  with  $\mathcal{S}(-z) = -\mathcal{S}(z)$  implies that points  $(\mathcal{C}(a), \mathcal{S}(a))$  and  $(\mathcal{C}(-b), \mathcal{S}(-b))$  are coincident points on the Cornu spiral in parametric form  $(\mathcal{C}(t), \mathcal{S}(t))$  and thus  $a = -b$ . Hence,

$$0 = a + b = \frac{A - \Delta\vartheta}{\sqrt{2\pi A}} + \frac{A + \Delta\vartheta}{\sqrt{2\pi A}} = \frac{\sqrt{2A}}{\sqrt{\pi}},$$

and thus  $A = 0$  which contradict the assumption that  $A > 0$ . The case with  $A < 0$  is similar.  $\square$

Actually, the situation can be understood graphically looking at the plots of  $g(A)$  and  $h(A)$ , as in figure 2 on the left. It is possible to reverse the implication by the following lemma.

LEMMA 3.3. *The solutions of the nonlinear system (6) are given by*

$$L = \frac{\sqrt{\Delta x^2 + \Delta y^2}}{h(A)}, \quad \kappa = \frac{\Delta\vartheta - A}{L}, \quad \kappa' = \frac{2A}{L^2}, \quad (12)$$

where  $A$  is a root of  $g(A)$  defined in equation (8) and  $h(A)$  is defined in (10).

PROOF. Let  $L, A$  satisfy (8) and (12). Then  $f(L, A) = 0$  and thus  $\mathbf{G}(L, A) = \mathbf{0}$ . From Lemma 3.2 when  $g(A) = 0$  then  $h(A) \neq 0$  and thus  $L$  is well defined.  $\square$

Remark 3.4. The solution of problem 1 is build using Lemma 3.3 selecting solution of minimal length. Notice that the parameter  $A$  corresponding to minimal (positive)  $L$  depend only on the *relative* angles and it is independent on scaling factor. So that we can compute  $A$  using only  $\Delta\varphi$  and  $\Delta\vartheta$  assuming  $r = \sqrt{\Delta x^2 + \Delta y^2} = 1$ .

Hence the interpolation problem is reduced to a single (nonlinear) equation that can be solved numerically with Newton–Raphson Method. By a graphical inspection we notice that the roots of  $g(A)$  are simple, so that Newton–Raphson converges quadratically. Function `findA` with `buildGrid` implements a simple strategy for the computation of minimum length clothoid on a grid of points and angles. This algorithm is used to compute surface presented in Figure 3 on the top.

<b>Function</b> <code>findA</code> ( $A_{\text{guess}}, \Delta\vartheta, \Delta\varphi, \text{tol}$ )
<pre> 1 Define <math>g</math> as <math>g(A) := \Theta(A, \Delta\vartheta, \Delta\varphi)</math>; Set <math>A \leftarrow A_{\text{guess}}</math>; 2 <b>while</b> <math> g(A)  &gt; \text{tol}</math> <b>do</b> <math>A \leftarrow A - g(A)/g'(A)</math>; 3 <b>return</b> <math>A</math>; </pre>
<b>Function</b> <code>buildGrid</code> ( $N, M$ )
<pre> 1 <b>for</b> <math>j = 0, 1, \dots, M</math> <b>do</b> <math>A_j^{\text{guess}} \leftarrow (j/M)40 - 20</math>; 2 <b>for</b> <math>i, j = 0, \dots, N</math> <b>do</b> 3   <math>\Delta\varphi \leftarrow 2\pi i/N - \pi</math>; <math>\Delta\vartheta \leftarrow 2\pi j/N - \pi</math>; <math>L_{ij} \leftarrow \infty</math>; 4   <b>for</b> <math>k = 1, \dots, M</math> <b>do</b> 5     <b>if</b> <math>\Theta(A_k^{\text{guess}}, \Delta\vartheta, \Delta\varphi) \Theta(A_{k-1}^{\text{guess}}, \Delta\vartheta, \Delta\varphi) \leq 0</math> <b>then</b> 6       <math>\tilde{A} \leftarrow \text{findA}((A_k^{\text{guess}} + A_{k-1}^{\text{guess}})/2, \Delta\vartheta, \Delta\varphi)</math>; 7       <math>\tilde{L} \leftarrow 1/\Theta(\tilde{A}, \Delta\vartheta, \Delta\varphi + \pi/2)</math>; 8       <b>if</b> <math>\tilde{L} &gt; 0</math> and <math>\tilde{L} &lt; L_{ij}</math> <b>then</b> <math>L_{ij} \leftarrow \tilde{L}</math>; <math>A_{ij} \leftarrow \tilde{A}</math>; 9     <b>end if</b> 10  <b>end for</b> 11 <b>end for</b> 12 <b>return</b> <math>A, L</math>; </pre>

In the next section a recipe to select a good initial point is described.

#### 4. SOLUTION OF $G^1$ HERMITE INTERPOLATION PROBLEM

By a graphical inspection the solution is in the range  $[-20, 20]$  for angles  $\Delta\varphi$  and  $\Delta\vartheta$  in the interval  $[-\pi, \pi]$ . The function `buildGrid` is used to compute all the possible solutions in this interval for angles ranging in  $[-\pi, \pi]$  and selecting the ones with minimum length. The strategy is very simple; the interval  $[-20, 20]$  is divided in small intervals and where  $g(A)$

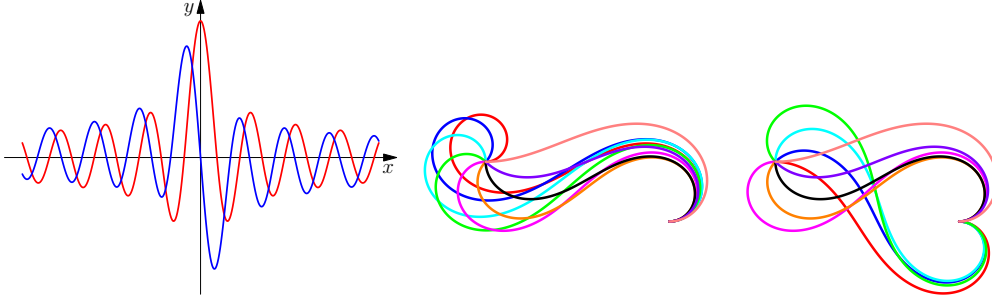


Fig. 2. On the left: plot of  $g$  (red line) and  $h$  (blue line), when  $g(A) = 0$  then  $h(A) \neq 0$  so that the length  $L$  is well defined. In centre clothoids computed using (13) as starting point for Newton-Raphson iterative scheme, on the right the minimum length clothoids. The clothoids start from  $(0, 0)$  angle 0 to  $(-0.95, 0.31)$  and angle ranging from  $-\pi$  to  $\pi$ .

changes sign Newton-Raphson iterative scheme is used. If convergence is attained and  $L$ , computed using (12), is positive, this solution is a candidate to be the final solution.

This strategy, although simple, is effective and permits to evaluate the solution of Problem 1 at any point. Figure 3 shows the results of computation using `buildGrid` with  $N = 32$  and  $M = 128$ . Notice that the solution is discontinuous for higher and lower angles. To avoid this jump in the solution we drop the requirement of minimal length for all angles and solve the following problem.

**PROBLEM 2.** *Given two points  $(x_0, y_0)$  and  $(x_1, y_1)$  and two angles  $\vartheta_0$  and  $\vartheta_1$ , find a clothoid segment of the form (1) which satisfies (2) with minimal positive  $L$  for  $|\vartheta_0|$  and  $|\vartheta_1|$  less than  $\pi/2$ . For greater angles we choose the solution that make the function  $\mathcal{A}(\Delta\vartheta, \Delta\varphi)$  with  $\mathcal{A}(\Delta\vartheta, \Delta\varphi) \in \{A \mid \Theta(A, \Delta\vartheta, \Delta\varphi) = 0\}$  a continuous surface.*

Looking at Figure 3 we guess that  $\mathcal{A}(\Delta\vartheta, \Delta\varphi)$  can be approximated by a plane. A simple fitting on the solution of Problem 2 with a plane, results in the following approximation for  $\mathcal{A}(\Delta\vartheta, \Delta\varphi)$ :

$$\mathcal{A}(\Delta\vartheta, \Delta\varphi) \approx 2.4674 \Delta\vartheta + 5.2478 \Delta\varphi. \quad (13)$$

Using (13) as starting point for Newton-Raphson the correct solution for Problem 2 is found in few iterations. Figure 3 show the computed solution found using this strategy. Computing the solution with Newton-Raphson starting with the guess given by (13) in a  $1024 \times 1024$  grid with a tolerance of  $10^{-10}$  results in the following iteration distribution:

iter	1	2	3	4	5
#cases	1	212	148880	846868	54664
		less than 1%	14%	80%	5%

Notice that the average number of iteration is 3.9 while the maximum number of iterations per point is 5. Figure 2 on the right shows the difference of computing minimum length clothoid curve and clothoid curve of Problem 2. The minimum length produces a bad looking solution for some angles combinations. The curve produced by the solution of Problem 2 looks better and in any case curve produced by the solution of Problem 1 and Problem 2 are identical for a large combination of points and angles.

The algorithm for the clothoid computation is resumed in function `buildClothoid` which uses `normalizeAngle` to put angles in the correct ranges.

**Function** `normalizeAngle( $\varphi$ )`

```

1 while  $\varphi > +\pi$  do  $\varphi \leftarrow \varphi - 2\pi$ ;
2 while  $\varphi < -\pi$  do  $\varphi \leftarrow \varphi + 2\pi$ ;
3 return  $\varphi$ ;

```

Function `buildClothoid` solves equation (8) that is it finds a solution of the equation  $g(A) = 0$  by calling `findA` described at the end of Section 3.

**Function** `buildClothoid( $x_0, y_0, \vartheta_0, x_1, y_1, \vartheta_1$ )`

```

1  $\Delta x \leftarrow x_1 - x_0$ ;  $\Delta y \leftarrow y_1 - y_0$ ;
2 Compute  $r$  and  $\varphi$  from  $r \cos \varphi = \Delta x$  and  $r \sin \varphi = \Delta y$ ;
3  $\Delta \varphi \leftarrow \text{normalizeAngle}(\vartheta_0 - \varphi)$ ;  $\Delta \vartheta \leftarrow \text{normalizeAngle}(\vartheta_1 - \vartheta_0)$ ;
4  $A \leftarrow \text{findA}(2.4674 \Delta \vartheta + 5.2478 \Delta \varphi, \Delta \vartheta, \Delta \varphi)$ ;
5  $L \leftarrow r / \Theta(A, \Delta \vartheta, \Delta \varphi + \frac{\pi}{2})$ ;  $\kappa \leftarrow (\Delta \vartheta - A) / L$ ;  $\kappa' \leftarrow (2A) / L^2$ ;
6 return  $\kappa, \kappa', L$ 

```

The algorithm needs accurate computation of Fresnel related functions  $g(A)$  and  $h(A)$  with relative derivative which are discussed in the next section.

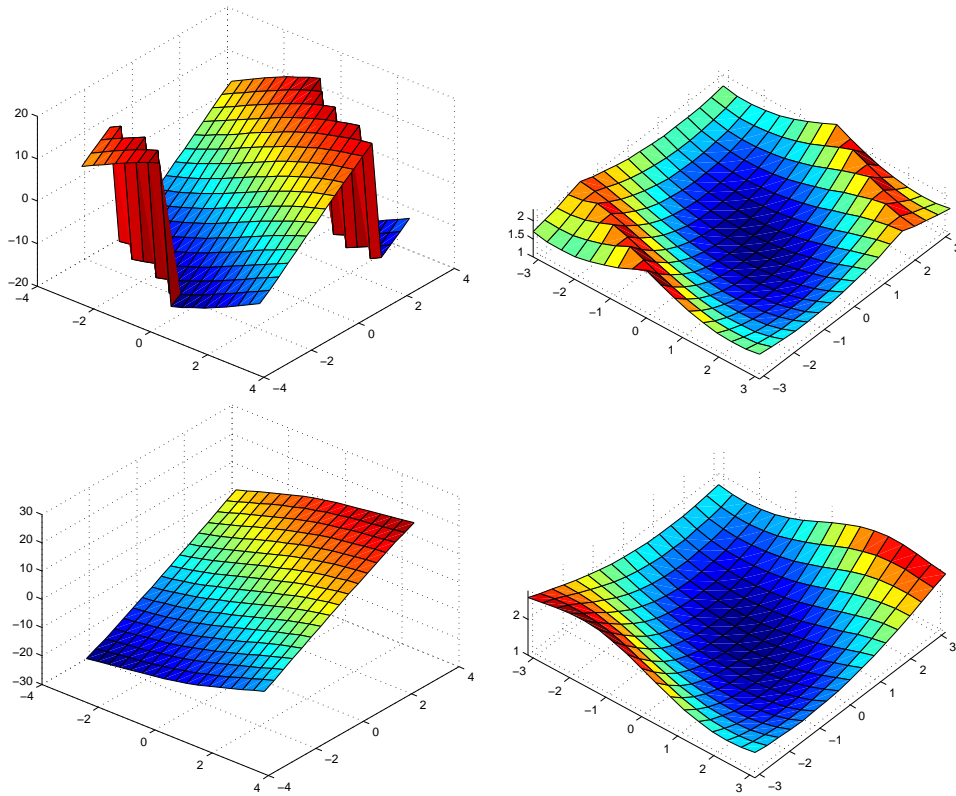


Fig. 3. On the top, computation of parameter  $A$  and minimal length and for nonlinear system (6). On the bottom computation of parameters  $A$  and  $L$  for Problem 2. Computation of the figures on the top are done using auxiliary function `buildGrid`.

## 5. COMPUTATION OF FRESNEL AND RELATED INTEGRALS

Among the various possible definitions, we choose the following one, which is the same adopted in Abramowitz and Stegun(1964).

*Definition 5.1 (Fresnel Integrals).* Following Abramowitz and Stegun(1964) the Fresnel Integrals are defined as

$$\mathcal{C}(t) = \int_0^t \cos\left(\frac{\pi}{2}\tau^2\right) d\tau, \quad \mathcal{S}(t) = \int_0^t \sin\left(\frac{\pi}{2}\tau^2\right) d\tau. \quad (14)$$

*Remark 5.2.* Some authors prefer the definition

$$\mathcal{C}(t) = \int_0^t \cos(\tau^2) d\tau, \quad \text{and} \quad \mathcal{S}(t) = \int_0^t \sin(\tau^2) d\tau.$$

However by using the identities

$$\int_0^t \cos(\tau^2) d\tau = \frac{\sqrt{\pi}}{\sqrt{2}} \int_0^{\frac{\sqrt{2}}{\sqrt{\pi}}t} \cos\left(\frac{\pi}{2}\tau^2\right) d\tau, \quad \int_0^t \sin(\tau^2) d\tau = \frac{\sqrt{\pi}}{\sqrt{2}} \int_0^{\frac{\sqrt{2}}{\sqrt{\pi}}t} \sin\left(\frac{\pi}{2}\tau^2\right) d\tau,$$

it is easy to pass between the two definitions.

To compute the standard Fresnel integrals one can use algorithms described in Snyder(1993), Smith(2011) and Thompson(1997) or using continued fraction expansion as in Backeljauw and Cuyt(2009). It is possible to reduce the integrals (1) to a linear combination of this standard Fresnel integrals (14). However simpler expression are obtained using also the momenta of the Fresnel integrals:

$$\mathcal{C}_k(t) = \int_0^t \tau^k \cos\left(\frac{\pi}{2}\tau^2\right) d\tau, \quad \mathcal{S}_k(t) = \int_0^t \tau^k \sin\left(\frac{\pi}{2}\tau^2\right) d\tau. \quad (15)$$

Notice that  $\mathcal{C}(t) := \mathcal{C}_0(t)$  and  $\mathcal{S}(t) := \mathcal{S}_0(t)$ . Closed forms via the exponential integral or the Gamma function are also possible, however we prefer to express them as a recurrence. Integrating by parts, the following recurrence is obtained:

$$\begin{aligned} \mathcal{C}_{k+1}(t) &= \frac{1}{\pi} \left( t^k \sin\left(\frac{\pi}{2}t^2\right) - k \mathcal{S}_{k-1}(t) \right), \\ \mathcal{S}_{k+1}(t) &= \frac{1}{\pi} \left( k \mathcal{C}_{k-1}(t) - t^k \cos\left(\frac{\pi}{2}t^2\right) \right). \end{aligned} \quad (16)$$

Recurrence is started by computing standard Fresnel integrals (14) and (by using the change of variable  $z = \tau^2$ ) the following values

$$\mathcal{C}_1(t) = \frac{1}{\pi} \sin\left(\frac{\pi}{2}t^2\right), \quad \mathcal{S}_1(t) = \frac{1}{\pi} \left( 1 - \cos\left(\frac{\pi}{2}t^2\right) \right),$$

From recurrence follows that  $\mathcal{C}_k(t)$  and  $\mathcal{S}_k(t)$  with  $k$  odd do not contain Fresnel integrals (14) and are combination of elementary functions.

The computation of clothoids relies most on the evaluation of integrals of kind (9) with their derivatives. The reduction is possible via a change of variable and integration by parts. It is enough to consider two integrals, that cover all possible cases:

$$\begin{aligned} X_k(a, b, c) &= \int_0^1 \tau^k \cos\left(\frac{a}{2}\tau^2 + b\tau + c\right) d\tau, \\ Y_k(a, b, c) &= \int_0^1 \tau^k \sin\left(\frac{a}{2}\tau^2 + b\tau + c\right) d\tau. \end{aligned} \quad (17)$$

In fact, integrals (8) and (10) with their derivatives can be evaluated by using the identity

$$\int_0^s \cos\left(\frac{1}{2}\kappa'\tau^2 + \kappa\tau + \vartheta_0\right) d\tau = s \int_0^1 \cos\left(\frac{a}{2}z^2 + bz + c\right) dz$$



where  $a = \kappa' s^2$ ,  $b = \kappa s$ , and  $c = \vartheta_0$  so that

$$g(\eta) = Y_0(2\eta, \Delta\vartheta - \eta, -\varphi), \quad h(\eta) = X_0(2\eta, \Delta\vartheta - \eta, -\varphi),$$

and finally, equation (1) can be evaluated as

$$\begin{aligned} x(s) &= x_0 + s X_0(\kappa' s^2, \kappa s, \vartheta_0), \\ y(s) &= y_0 + s Y_0(\kappa' s^2, \kappa s, \vartheta_0). \end{aligned}$$

From now on, algorithms for accurate computation of  $X_k$  and  $Y_k$  are discussed. From the well known identities

$$\cos(\alpha + \beta) = \cos \alpha \cos \beta - \sin \alpha \sin \beta, \quad \sin(\alpha + \beta) = \sin \alpha \cos \beta + \cos \alpha \sin \beta, \quad (18)$$

integrals (17) can be rewritten as

$$\begin{aligned} X_k(a, b, c) &= X_k(a, b, 0) \cos c - Y_k(a, b, 0) \sin c, \\ Y_k(a, b, c) &= X_k(a, b, 0) \sin c + Y_k(a, b, 0) \cos c, \end{aligned}$$

Thus defining  $X_k(a, b) := X_k(a, b, 0)$  and  $Y_k(a, b) := Y_k(a, b, 0)$  the computation of (17) is reduced to the computation of  $X_k(a, b)$  and  $Y_k(a, b)$ . It is convenient to introduce the following quantities

$$s = \frac{a}{|a|}, \quad z = \frac{\sqrt{|a|}}{\sqrt{\pi}}, \quad \ell = \frac{sb}{\sqrt{\pi|a|}}, \quad \gamma = -\frac{sb^2}{2|a|},$$

so that it is possible to rewrite the argument of the trigonometric functions of  $X_k(a, b)$  and  $Y_k(a, b)$  as

$$\frac{a}{2}\tau^2 + b\tau = \frac{\pi}{2}s \left( \tau \frac{\sqrt{|a|}}{\sqrt{\pi}} + \frac{sb}{\sqrt{\pi|a|}} \right)^2 - \frac{sb^2}{2|a|} = \frac{\pi}{2}s(\tau z + \ell)^2 + \gamma.$$

By using the change of variable  $\xi = \tau z + \ell$  with inverse  $\tau = z^{-1}(\xi - \ell)$  for  $X_k(a, b)$  and the identity (18) we have:

$$\begin{aligned} X_k(a, b) &= z^{-1} \int_{\ell}^{\ell+z} z^{-k} (\xi - \ell)^k \cos \left( \frac{s\pi}{2} \xi^2 + \gamma \right) d\xi, \\ &= z^{-k-1} \int_{\ell}^{\ell+z} \sum_{j=0}^k \binom{k}{j} \xi^j \ell^{k-j} \cos \left( \frac{s\pi}{2} \xi^2 + \gamma \right) d\xi, \\ &= z^{-k-1} \sum_{j=0}^k \binom{k}{j} \ell^{k-j} [\cos \gamma \Delta \mathcal{C}_j - s \sin \gamma \Delta \mathcal{S}_j], \end{aligned}$$

where

$$\Delta \mathcal{C}_j = \mathcal{C}_j(\ell + z) - \mathcal{C}_j(\ell), \quad \Delta \mathcal{S}_j = \mathcal{S}_j(\ell + z) - \mathcal{S}_j(\ell), \quad (19)$$

are the evaluation of the momenta of the Fresnel integrals as defined in (15). Analogously for  $Y_k(a, b)$  we have:

$$Y_k(a, b) = z^{-k-1} \sum_{j=0}^k \binom{k}{j} \ell^{k-j} [\sin \gamma \Delta \mathcal{C}_j + s \cos \gamma \Delta \mathcal{S}_j].$$

A cheaper way to compute  $X_k(a, b)$  and  $Y_k(a, b)$  is via recurrence as in (16) for the computation of Fresnel momenta. Integrating the identity,

$$\frac{d}{dt} \left[ t^k \sin \left( \frac{a}{2} t^2 + bt \right) \right] = kt^{k-1} \sin \left( \frac{a}{2} t^2 + bt \right) + t^k (at + b) \cos \left( \frac{a}{2} t^2 + bt \right)$$

we have

$$\sin\left(\frac{a}{2} + b\right) = kY_{k-1}(a, b) + aX_{k+1}(a, b) + bX_k(a, b)$$

which can be solved for  $X_{k+1}(a, b)$ . Repeating the same argument with  $\cos((a/2)t^2 + bt)$  and solving for  $Y_{k+1}(a, b)$  we obtain recurrences for  $X$  and  $Y$ :

$$\begin{aligned} X_{k+1}(a, b) &= \frac{1}{a} \left( \sin\left(\frac{a}{2} + b\right) - bX_k(a, b) - kY_{k-1}(a, b) \right), \\ Y_{k+1}(a, b) &= \frac{1}{a} \left( kX_{k-1}(a, b) - bY_k(a, b) - \cos\left(\frac{a}{2} + b\right) \right). \end{aligned} \quad (20)$$

From the identities

$$\begin{aligned} \int_0^1 (a\tau + b) \cos\left(\frac{a}{2}\tau^2 + b\tau\right) d\tau &= aX_1(a, b) + bX_0(a, b) = \sin\left(\frac{a}{2} + b\right), \\ \int_0^1 (a\tau + b) \sin\left(\frac{a}{2}\tau^2 + b\tau\right) d\tau &= aY_1(a, b) + bY_0(a, b) = 1 - \cos\left(\frac{a}{2} + b\right), \end{aligned}$$

it follows

$$\begin{aligned} X_1(a, b) &= \frac{1}{a} \left( \sin\left(\frac{a}{2} + b\right) - bX_0(a, b) \right), \\ Y_1(a, b) &= \frac{1}{a} \left( 1 - \cos\left(\frac{a}{2} + b\right) - bY_0(a, b) \right). \end{aligned} \quad (21)$$

To complete recurrence we need the initial values  $X_0(a, b)$ ,  $Y_0(a, b)$ :

$$\begin{aligned} X_0(a, b) &= z^{-1} (\cos \gamma \Delta \mathcal{C}_0 - s \sin \gamma \Delta \mathcal{S}_0), \\ Y_0(a, b) &= z^{-1} (\sin \gamma \Delta \mathcal{C}_0 + s \cos \gamma \Delta \mathcal{S}_0), \end{aligned} \quad (22)$$

where  $\mathcal{C}_0$  and  $\mathcal{S}_0$  is defined in (19). This recurrence may be inaccurate when  $|a|$  is small, in fact  $z$  appears in the denominator of many fractions. For this reason for small values of  $|a|$  we substitute this recurrence with asymptotic expansions.

## 6. ACCURATE COMPUTATION WITH SMALL PARAMETERS

When the parameter  $a$  is small we use identity (18) to derive series expansion

$$\begin{aligned} X_k(a, b) &= \int_0^1 \tau^k \cos\left(\frac{a}{2}\tau^2 + b\tau\right) d\tau \\ &= \int_0^1 \tau^k \left[ \cos\left(\frac{a}{2}\tau^2\right) \cos(b\tau) - \sin\left(\frac{a}{2}\tau^2\right) \sin(b\tau) \right] d\tau \\ &= \sum_{n=0}^{\infty} \frac{(-1)^n}{(2n)!} \left(\frac{a}{2}\right)^{2n} X_{4n+k}(0, b) - \sum_{n=0}^{\infty} \frac{(-1)^n}{(2n+1)!} \left(\frac{a}{2}\right)^{2n+1} Y_{4n+2+k}(0, b) \\ &= \sum_{n=0}^{\infty} \frac{(-1)^n}{(2n)!} \left(\frac{a}{2}\right)^{2n} \left[ X_{4n+k}(0, b) - \frac{a Y_{4n+2+k}(0, b)}{2(2n+1)} \right] \end{aligned} \quad (23)$$

and analogously using again identity (18) we have the series expansion

$$\begin{aligned} Y_k(a, b) &= \int_0^1 \tau^k \sin\left(\frac{a}{2}\tau^2 + b\tau\right) d\tau \\ &= \sum_{n=0}^{\infty} \frac{(-1)^n}{(2n)!} \left(\frac{a}{2}\right)^{2n} \left[ Y_{4n+k}(0, b) + \frac{a X_{4n+2+k}(0, b)}{2(2n+1)} \right] \end{aligned} \quad (24)$$

From the inequalities

$$|X_k| \leq \int_0^1 |\tau^k| d\tau = \frac{1}{k+1}, \quad |Y_k| \leq \int_0^1 |\tau^k| d\tau = \frac{1}{k+1},$$

we can estimate the remainder for the series of  $X_k$

$$\begin{aligned} R_{p,k} &= \left| \sum_{n=p}^{\infty} \frac{(-1)^n}{(2n)!} \left(\frac{a}{2}\right)^{2n} \left[ X_{4n+k}(0, b) - \frac{a Y_{4n+2+k}(0, b)}{2(2n+1)} \right] \right| \\ &\leq \sum_{n=p}^{\infty} \frac{1}{(2n)!} \left(\frac{a}{2}\right)^{2n} \left[ \frac{1}{4n+1} + \frac{|a|}{2(2n+1)(4n+3)} \right] \\ &\leq \left(\frac{a}{2}\right)^{2p} \sum_{n=p}^{\infty} \frac{1}{(2(n-p))!} \left(\frac{a}{2}\right)^{2(n-p)} \\ &\leq \left(\frac{a}{2}\right)^{2p} \sum_{n=0}^{\infty} \frac{1}{(2n)!} \left(\frac{a}{2}\right)^{2n} = \left(\frac{a}{2}\right)^{2p} \cosh(a). \end{aligned}$$

The same estimate is obtained for the series of  $Y_k$

*Remark 6.1.* Series (23) and (24) converge fast. For example if  $|a| < 10^{-4}$  and  $p = 2$  the error is less than  $6.26 \cdot 10^{-18}$  while if  $p = 3$  the error is less than  $1.6 \cdot 10^{-26}$ .

Recurrence (20)-(21)-(22) permits to compute  $X_k(a, b)$  and  $Y_k(a, b)$  at arbitrary precision when  $a \neq 0$ , but when  $a = 0$  it modifies to

$$\begin{aligned} X_k(0, b) &= b^{-1}(\sin b - k Y_{k-1}(0, b)), \\ Y_k(0, b) &= b^{-1}(k X_{k-1}(0, b) - \cos b), \end{aligned} \quad (25)$$

with starting point

$$X_0(0, b) = b^{-1} \sin b, \quad Y_0(0, b) = b^{-1}(1 - \cos b).$$

Recurrence (25) with (23) and (24) permits computation when  $b \neq 0$ , unfortunately recurrence (25) is highly unstable and cannot be used. In alternative an explicit formula based on Lommel function  $s_{\mu, \nu}(z)$  can be used [Shirley and Chang(2003)]. Explicit formula is the following

$$\begin{aligned} X_k(0, b) &= \frac{k s_{k+\frac{1}{2}, \frac{3}{2}}(b) \sin b + f(b) s_{k+\frac{3}{2}, \frac{1}{2}}(b)}{(1+k)b^{k+\frac{1}{2}}} + \frac{\cos b}{1+k}, \\ Y_k(0, b) &= \frac{k s_{k+\frac{3}{2}, \frac{3}{2}}(b) \sin b + g(b) s_{k+\frac{1}{2}, \frac{1}{2}}(b)}{(2+k)b^{k+\frac{1}{2}}} + \frac{\sin b}{2+k}, \end{aligned} \quad (26)$$

where  $f(b) = b^{-1} \sin b - \cos b$  and  $g(b) = f(b)(2+k)$ . Lommel function has the following expansion (see <http://dlmf.nist.gov/11.9>)

$$s_{\mu, \nu}(z) = z^{\mu+1} \sum_{n=0}^{\infty} \frac{(-z^2)^n}{\alpha_{n+1}(\mu, \nu)}, \quad \alpha_n(\mu, \nu) = \prod_{m=1}^n ((\mu + 2m - 1)^2 - \nu^2), \quad (27)$$

and using this expansion in (26) results in the following explicit formula

$$\begin{aligned} X_k(0, b) &= A(b) w_{k+\frac{1}{2}, \frac{3}{2}}(b) + B(b) w_{k+\frac{3}{2}, \frac{1}{2}}(b) + \frac{\cos b}{1+k}, \\ Y_k(0, b) &= C(b) w_{k+\frac{3}{2}, \frac{3}{2}}(b) + D(b) w_{k+\frac{1}{2}, \frac{1}{2}}(b) + \frac{\sin b}{2+k}, \end{aligned}$$

where

$$w_{\mu,\nu}(b) = \sum_{n=0}^{\infty} \frac{(-b^2)^n}{\alpha_{n+1}(\mu,\nu)}, \quad A(b) = \frac{kb \sin b}{1+k}, \quad B(b) = \frac{(\sin b - b \cos b)b}{1+k},$$

$$C(b) = -\frac{b^2 \sin b}{2+k}, \quad D(b) = \sin b - b \cos b.$$

## 7. CONCLUDING REMARKS

The proposed algorithm is detailed in the appendix using pseudocode and can be easily translated in any programming language. A MATLAB implementation is furnished to test the functions introduced in the paper. It is important that the computation of Fresnel integrals is accurate because they are involved in many expansions for the clothoid fitting. In the MATLAB implementation of the proposed algorithm for Fresnel integrals approximation a slightly modified version of Venkata Sivakanth Telasula script, available in MATLAB Central, was used.

### A. ALGORITHMS FOR THE COMPUTATION OF FRESNEL RELATED INTEGRALS

We present here the algorithmic version of the analytical expression we derived in Section 5 and 6. This algorithm are necessary for the computation of the main function `buildClothoid` of Section 4 which takes the input data  $(x_0, y_0, \vartheta_0, x_1, y_1, \vartheta_1)$  and returns the parameters  $(\kappa, \kappa', L)$  that solve the problem as expressed in equation (1). Function `evalXY` computes the generalized Fresnel integrals (17). It distinguishes the cases of  $a$  larger or smaller than a threshold  $\varepsilon$ . The value of  $\varepsilon$  is discussed in Section 6, see for example Remark 6.1. Formulas (20)-(21)-(22), used to compute  $X_k(a, b)$  and  $Y_k(a, b)$  at arbitrary precision when  $|a| \geq \varepsilon$ , are implemented in function `evalXYaLarge`. Formulas (23)-(24), used to compute  $X_k(a, b)$  and  $Y_k(a, b)$  at arbitrary precision when  $|a| < \varepsilon$ , are implemented in function `evalXYaSmall`. This function requires computation of (25) and (26) implemented in function `evalXYaZero` which needs (reduced) Lommel function (27) implemented in function `rLommel`.

#### Function `evalXY(a, b, c, k)`

```

1 if  $|a| < \varepsilon$  then  $X^0, Y^0 \leftarrow \text{evalXYaSmall}(a, b, k, p)$ ; else  $X^0, Y^0 \leftarrow \text{evalXYaLarge}(a, b, k)$ ;
2 for  $j = 0, 1, \dots, k$  do
3    $X_j \leftarrow X_j^0 \cos c - Y_j^0 \sin c$ ;  $Y_j \leftarrow X_j^0 \sin c + Y_j^0 \cos c$ ;
4 end for
5 return  $X, Y$ 

```

## References

- Abramowitz, M., Stegun, I. A. (Eds.), 1964. Handbook of Mathematical Functions with Formulas, Graphs, and Mathematical Tables. No. 55 in National Bureau of Standards Applied Mathematics Series. U.S. Government Printing Office, Washington, D.C., corrections appeared in later printings up to the 10th Printing, December, 1972. Reproductions by other publishers, in whole or in part, have been available since 1965.
- Backeljauw, F., Cuyt, A., Jul. 2009. Algorithm 895: A continued fractions package for special functions. ACM Trans. Math. Softw. 36 (3), 15:1–15:20.  
URL <http://doi.acm.org/10.1145/1527286.1527289>
- Baran, I., Lehtinen, J., Popović, J., May 2010. Sketching clothoid splines using shortest paths. Computer Graphics Forum 29 (2), 655–664.
- Davis, T., NOV 1999. Total least-squares spiral curve fitting. JOURNAL OF SURVEYING ENGINEERING-ASCE 125 (4), 159–176.
- De Boor, C., 1978. A Practical Guide to Splines. No. v. 27 in Applied Mathematical Sciences. Springer-Verlag.  
URL <http://books.google.it/books?id=mZMQAQAAIAAJ>

**Function evalXYaLarge( $a, b, k$ )**

```

1  $s \leftarrow \frac{a}{|a|}$ ;  $z \leftarrow \frac{\sqrt{\pi}}{\sqrt{|a|}}$ ;  $\ell \leftarrow \frac{sb}{z\pi}$ ;  $\gamma \leftarrow -\frac{sb^2}{2|a|}$ ;  $t \leftarrow \frac{1}{2}a + b$ ;
2  $\Delta\mathcal{C}_0 \leftarrow \mathcal{C}(\ell + z) - \mathcal{C}(\ell)$ ;
3  $\Delta\mathcal{S}_0 \leftarrow \mathcal{S}(\ell + z) - \mathcal{S}(\ell)$ ;
4  $X_0 \leftarrow z^{-1}(\cos \gamma \Delta\mathcal{C}_0 - s \sin \gamma \Delta\mathcal{S}_0)$ ;
5  $Y_0 \leftarrow z^{-1}(\sin \gamma \Delta\mathcal{C}_0 + s \cos \gamma \Delta\mathcal{S}_0)$ ;
6  $X_1 \leftarrow a^{-1}(\sin t - bX_0)$ ;
7  $Y_1 \leftarrow a^{-1}(1 - \cos t - bY_0)$ ;
8 for  $j = 1, 2, \dots, k - 1$  do
9    $X_{j+1} \leftarrow a^{-1}(\sin t - bX_j - jY_{j-1})$ ;
10   $Y_{j+1} \leftarrow a^{-1}(jX_{j-1} - bY_j - \cos t)$ ;
11 end for
12 return  $X, Y$ 

```

**Function rLommel( $\mu, \nu, b$ )**

```

1  $t \leftarrow (\mu + \nu + 1)^{-1}(\mu - \nu + 1)^{-1}$ ;  $r \leftarrow t$ ;  $n \leftarrow 1$ ;
2 while  $|t| > \varepsilon$  do  $t \leftarrow t \frac{(-b)}{2n + \mu - \nu + 1} \frac{b}{2n + \mu + \nu + 1}$ ;  $r \leftarrow r + t$ ;  $n \leftarrow n + 1$ ;
3 return  $r$ 

```

**Function evalXYaZero( $b, k$ )**

```

1 if  $|b| < \varepsilon$  then
2    $X_0 \leftarrow 1 - \frac{b^2}{6} \left(1 - \frac{b^2}{20}\right)$ ;  $Y_0 \leftarrow \frac{b^2}{2} \left(1 - \frac{b^2}{6} \left(1 - \frac{b^2}{30}\right)\right)$ ;
3 else
4    $X_0 \leftarrow \frac{\sin b}{b}$ ;  $Y_0 \leftarrow \frac{1 - \cos b}{b}$ ;
5 end if
6  $A \leftarrow b \sin b$ ;  $D \leftarrow \sin b - b \cos b$ ;  $B \leftarrow bD$ ;  $C \leftarrow -b^2 \sin b$ ;
7 for  $k = 0, 1, \dots, k - 1$  do
8    $X_{k+1} \leftarrow \frac{kA \text{rLommel}\left(k + \frac{1}{2}, \frac{3}{2}, b\right) + B \text{rLommel}\left(k + \frac{3}{2}, \frac{1}{2}, b\right) + \cos b}{1 + k}$ ;
9    $Y_{k+1} \leftarrow \frac{C \text{rLommel}\left(k + \frac{3}{2}, \frac{3}{2}, b\right) + \sin b}{2 + k} + D \text{rLommel}\left(k + \frac{1}{2}, \frac{1}{2}, b\right)$ ;
10 end for
11 return  $X, Y$ 

```

De Cecco, M., Bertolazzi, E., Miori, G., Oboe, R., Baglivo, L., 2007. Pc-sliding for vehicles path planning and control - design and evaluation of robustness to parameters change and measurement uncertainty. In: ICINCO-RA (2)'2007. pp. 11-18.

Farin, G., 2002. Curves and surfaces for CAGD: a practical guide, 5th Edition. Morgan Kaufmann Publishers Inc., San Francisco, CA, USA.

Farouki, R. T., Neff, C. A., Oct. 1995. Hermite interpolation by pythagorean hodograph quintics. Math. Comput. 64 (212), 1589-1609.  
URL <http://dx.doi.org/10.2307/2153373>

Function evalXYaSmall( $a, b, k, p$ )	
1	$X^0, Y^0 \leftarrow \text{evalXYaZero}(b, k + 4p + 2); \quad t \leftarrow 1;$
2	<b>for</b> $j = 0, 1, \dots, k$ <b>do</b> $X_j \leftarrow X_j^0 - \frac{a}{2} Y_{j+2}^0; \quad Y_j \leftarrow Y_j^0 + \frac{a}{2} X_{j+2}^0;$
3	<b>for</b> $n = 1, 2, \dots, p$ <b>do</b>
4	$t \leftarrow \frac{-t a^2}{16n(2n-1)};$
5	<b>for</b> $j = 0, 1, \dots, k$ <b>do</b>
6	$X_j \leftarrow X_j + t \frac{X_{4n+j}^0 - a Y_{4n+j+2}^0}{4n+2}; \quad Y_j \leftarrow Y_j + t \frac{Y_{4n+j}^0 + a X_{4n+j+2}^0}{4n+2};$
7	<b>end for</b>
8	<b>end for</b>
9	<b>return</b> $X, Y$

- McCrae, J., Singh, K., Jun. 2009. Sketching piecewise clothoid curves. *Computers & Graphics*.  
 URL <http://dx.doi.org/10.1016/j.cag.2009.05.006>
- Meek, D. S., Walton, D. J., Jul. 1992. Clothoid spline transition spirals. *Mathematics of Computation* 59, 117–133.
- Meek, D. S., Walton, D. J., Sep. 2004. A note on finding clothoids. *J. Comput. Appl. Math.* 170 (2), 433–453.  
 URL <http://dx.doi.org/10.1016/j.cam.2003.12.047>
- Meek, D. S., Walton, D. J., Jan. 2009. A two-point g1 hermite interpolating family of spirals. *J. Comput. Appl. Math.* 223 (1), 97–113.  
 URL <http://dx.doi.org/10.1016/j.cam.2007.12.027>
- Pavlidis, T., Jan. 1983. Curve fitting with conic splines. *ACM Trans. Graph.* 2 (1), 1–31.  
 URL <http://doi.acm.org/10.1145/357314.357315>
- Scheuer, A., Fraichard, T., sep 1997. Continuous-curvature path planning for car-like vehicles. In: *Intelligent Robots and Systems, 1997. IROS '97., Proceedings of the 1997 IEEE/RSJ International Conference on*. Vol. 2. pp. 997–1003 vol.2.
- Shirley, E. L., Chang, E. K., 2003. Accurate efficient evaluation of lommel functions for arbitrarily large arguments. *Metrologia* 40 (1), S5.  
 URL <http://stacks.iop.org/0026-1394/40/i=1/a=302>
- Smith, D. M., Feb. 2011. Algorithm 911: Multiple-precision exponential integral and related functions. *ACM Trans. Math. Softw.* 37 (4), 46:1–46:16.  
 URL <http://doi.acm.org/10.1145/1916461.1916470>
- Snyder, W. V., Dec. 1993. Algorithm 723: Fresnel integrals. *ACM Transactions on Mathematical Software* 19 (4), 452–456.  
 URL <http://doi.acm.org/10.1145/168173.168193>
- Thompson, W. J., 1997. *Atlas for Computing Mathematical Functions: An Illustrated Guide for Practitioners with Programs in C and Mathematica with Cdrom*, 1st Edition. John Wiley & Sons, Inc., New York, NY, USA.
- Walton, D., Meek, D., 1996. A planar cubic bezier spiral. *Journal of Computational and Applied Mathematics* 72 (1), 85–100.  
 URL <http://www.sciencedirect.com/science/article/pii/0377042795002464>
- Walton, D., Meek, D., 2009. Interpolation with a single cornu spiral segment. *Journal of Computational and Applied Mathematics* 223 (1), 86–96.  
 URL <http://www.sciencedirect.com/science/article/pii/S037704270700670X>
- Walton, D. J., Meek, D. S., Jul. 2007. G2 curve design with a pair of pythagorean hodograph quintic spiral segments. *Comput. Aided Geom. Des.* 24 (5), 267–285.  
 URL <http://dx.doi.org/10.1016/j.cagd.2007.03.003>